

Adsorbate-substrate vibrational coupling in physisorbed Kr films on Pt(111)

Klaus Kern, Peter Zeppenfeld, Rudolf David, and George Comsa
*Institut für Grenzflächenforschung und Vakuumphysik, Kernforschungsanlage Jülich,
 5170 Jülich, West Germany*

(Received 17 October 1986)

Surface-phonon dispersion curves have been measured by inelastic He scattering for thin Kr films (1, 2, 3, and 25 monolayers) physisorbed on Pt(111) along the $(\bar{\Gamma}\bar{K})_{\text{Kr}}$ azimuth. Phonon hybridization between the localized adlayer modes and the substrate Rayleigh wave is observed in the intersection region. Radiative damping causes a substantial phonon-linewidth broadening over the whole range where the adlayer modes overlap the substrate bulk bands.

Vibrational coupling between adsorbate and substrate is relevant for dynamical surface processes like scattering, accommodation, adsorption, desorption, or diffusion. One particular manifestation of this coupling is the linewidth broadening of the adsorbate vibrational modes. The main coupling mechanisms are through excitation of substrate phonons¹ or electron-hole pairs.² Experimental linewidths of adsorbate-substrate modes of chemisorbed overlayers on well characterized single-metal-crystal surfaces³ have been studied intensively during the last few years. In all these cases, the frequency of the adsorbate mode was well above the highest phonon frequency of the substrate, and nonradiative damping by electron-hole pair excitation was found to be the dominant energy relaxation process.

In the case of physisorbed adlayers, the situation is different. The physisorption potential is rather flat and broad, i.e., the restoring force of the vertical motion of the adatoms is weak, and thus the corresponding adsorbate-substrate vibrations are low-frequency modes.⁴⁻⁶ At the zone boundary of the surface Brillouin zone (BZ) these modes lie well below the substrate modes. Approaching the zone center, the adlayer mode inevitably intersects the substrate Rayleigh dispersion curve, and mode hybridization is expected.⁷ Finally, close to the zone center, the adlayer mode and the projected substrate bulk bands overlap. The adlayer phonon is thus no longer a real eigenmode and radiative damping into the substrate bulk phonon bands should lead to lifetime shortening and thus to linewidth broadening.⁷ A linewidth broadening in the first half of the BZ and a phonon intensity increase in the crossover region, which was ascribed to hybridization, have been observed by Gibson and Sibener⁸ for Xe monolayers on Ag(111).

We report here on a high-resolution inelastic He scattering study of the adsorbate-substrate phonon coupling in mono-, bi-, and trilayer films (ML, BL, and TL) of Kr physisorbed on Pt(111). Because of the high resolution and the good quality of the substrate surface the hybridization-induced splitting and intensity enhancement could be observed in detail. Likewise, the radiative-damping-induced linewidth broadening with a cutoff at the substrate bulk band edge has been observed for both the ML and BL samples.

The experimental details of the high-resolution He scattering apparatus have been discussed elsewhere;⁹ here

only the features relevant to the present experiment are given. The apparatus consists of a He nozzle beam source, a ultrahigh-vacuum target chamber, and a time-of-flight (TOF) detector line; the total scattering angle is fixed, i.e., $\theta_i + \theta_f = 90^\circ$. The energy of the incident He beam used here was $E = 18.3$ meV and the energy spread (full width at half maximum) $\Delta E/E \approx 1.4\%$. TOF analysis of the scattered He beam is performed by means of pseudorandom chopping with 2.5 μs time resolution (flight path 790 mm). The overall instrumental energy resolution of the TOF spectrometer is 2.1%.⁹ The angular spread of the incident beam and the angle subtended by the ionizer opening are both equal to 0.2° . The sample is a high-quality Pt(111) surface with an average terrace width of about 3000 Å.¹⁰ The surface phonon dispersion of the clean Pt(111) surface has been measured and these results have been published elsewhere.¹¹

The Kr films investigated here are obtained by exposing the Pt surface ($T_s = 25$ K) to a three-dimensional (3D) Kr pressure of $\sim 5 \times 10^{-8}$ mbar. When the desired coverage was reached, the 3D Kr was pumped off. The adsorbed layers were carefully annealed until an optimum equilibrium structure was obtained. By means of a procedure described in detail in Ref. 6 we could show that Kr, like Xe, wets completely the clean Pt(111) surface; we could further ascertain that the Kr mono-, bi-, and trilayers used in the present experiment were complete within a few percent. The structure of the Kr films (1, 2, 3, and 25 monolayers) has been characterized by means of He diffraction. On the clean Pt(111) substrate Kr is found to form hexagonal overlayers which are rotated by 30° with respect to the symmetry axes of the substrate.¹² Figure 1 shows He-diffraction polar scans which are measured with the scattering plane oriented along the $\bar{\Gamma}\bar{M}$ direction of the Kr lattice, i.e., the $\bar{\Gamma}\bar{K}$ direction of the Pt(111) surface. The lattice constants of the ML and of the multilayers as deduced from the peak positions in Fig. 1 are 4.00 ± 0.02 and 3.96 ± 0.02 Å, respectively. From the polar peak widths an average domain size of ~ 250 Å is estimated, documenting the high quality of the various Kr layers.

Figure 2 shows a series of TOF spectra of the Kr monolayer taken along the $(\bar{\Gamma}\bar{K})_{\text{Kr}}$ azimuth with the abscissae transformed to an energy transfer scale. A least-squares fitting of the peaks with Gaussian distributions has been performed in order to determine unbiased peak positions

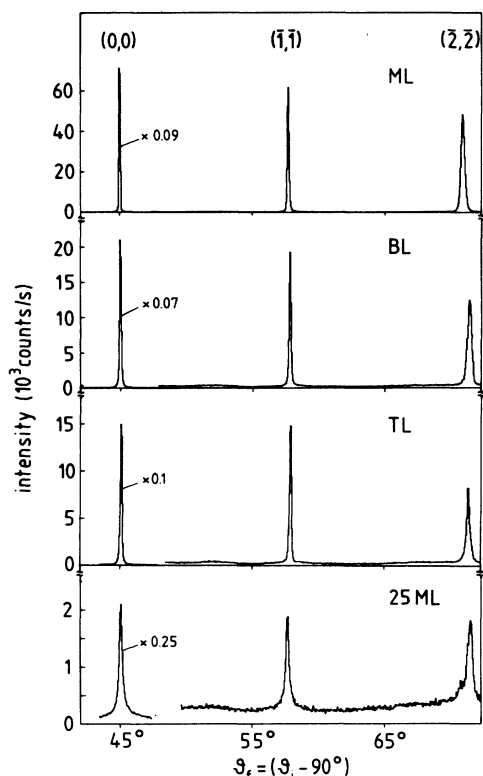


FIG. 1. Polar He-diffraction patterns of mono-, bi-, tri-, and 25-layer Kr films physisorbed on Pt(111) along the $(\bar{\Gamma}\bar{M})_{\text{Kr}}$ azimuth. All patterns were taken with a He-beam energy of 18.3 meV at $T_s = 25$ K.

and linewidths. The features in Fig. 2 are assigned as follows [we refer in particular to Fig. 2(a), where the features are well separated]. The peak at zero energy exchange is due to diffuse elastic scattering from residual surface impurities and defects, providing information on the surface quality.⁶ The largest peak at $\Delta E \approx -3.9$ meV corresponds to the creation of a Kr-monolayer phonon (vertical Kr-Pt vibration). Its counterpart, the phonon annihilation peak at $\Delta E \approx 3.7$ meV is much weaker due to the low surface temperature. Whether the peak at $\Delta E \approx -7.3$ meV corresponds to an overtone or to the creation of two phonons of the Kr monolayer cannot be unequivocally inferred from the present data. Of particular interest is the weak structure at $\Delta E \approx -3.1$ meV, close to the position of the Pt substrate Rayleigh wave. Note that this structure is seen in spite of the Kr monolayer being complete.

The plots in Fig. 2 taken at decreasing angle of incidence (increasing phonon wave vector Q) demonstrate strikingly the effect of both the hybridization between the Pt substrate Rayleigh wave and the Kr Einstein mode around their intersection [Figs. 2(b) and 2(c)] as well as the radiative damping of the Kr mode into the substrate bulk bands [compare Figs. 2(a) and 2(d)]; the effects occur as predicted by Hall, Mills, and Black.⁷ Indeed, the Pt substrate phonon feature which has a small intensity far from the intersection with the Kr mode [Fig. 2(a)] in-

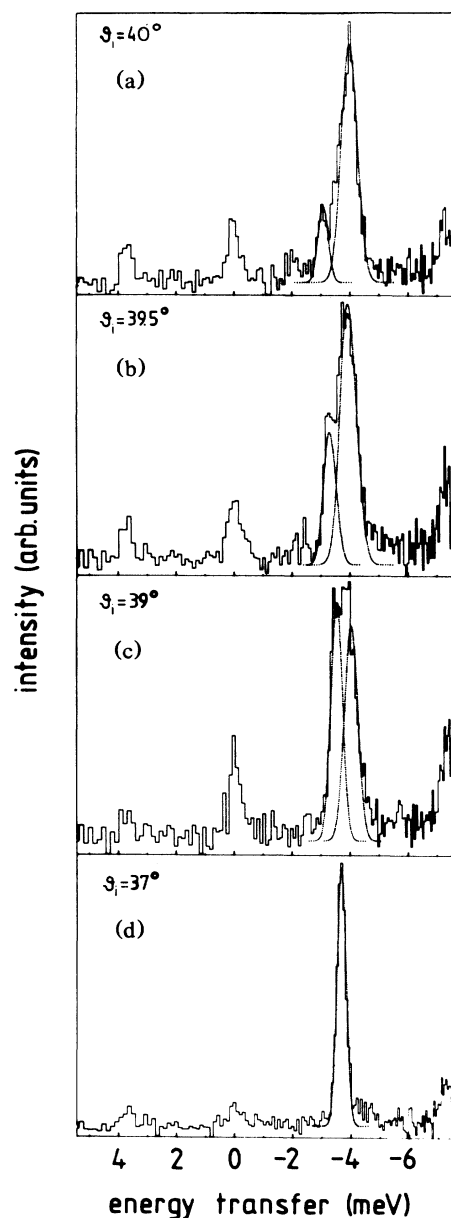


FIG. 2. He TOF spectra taken from a Kr monolayer along the $(\bar{\Gamma}\bar{K})_{\text{Kr}}$ azimuth at four different incident angles θ_i : (a) 40° , (b) 39.5° , (c) 39° , (d) 37° . With decreasing incident angles phonons with larger wave vector are probed. All spectra are transferred to an energy transfer scale; other experimental parameters like in Fig. 1.

creases dramatically due to the hybridization when approaching the intersection [Fig. 2(b)], leading eventually at the intersection to a doublet of nearly equal intensity [Fig. 2(c)]. With further wave-vector increase the higher-energy branch of the doublet vanishes abruptly and only a sharp Kr feature is present up to the zone boundary [Fig. 2(d)]. The substantial broadening of the Kr feature linewidth near the $\bar{\Gamma}$ point [Fig. 2(a)] with respect to the linewidth near the \bar{K} point [Fig. 2(d)] corresponds to the

lifetime reduction due to the radiative damping into the bulk bands.

The dispersion of the Kr mode (including the doublet feature around the intersection with the Pt substrate Rayleigh wave) obtained from a large number of spectra like those in Fig. 2 for mono-, bi-, and trilayer Kr films are plotted in Figs. 3(a), 3(b), and 3(c). The anomaly in the dispersion of the Kr-monolayer mode which is due to the coupling with the substrate Rayleigh wave appears to range between $Q \approx 0.25$ and 0.50 \AA^{-1} . It is noteworthy that the anomaly is likewise present in the bi- and even the trilayer films; the splitting of the doublet being reduced. It is especially the Q range of the anomaly, which becomes smaller and of course its location shifts towards smaller Q values together with the location of the intersection between the Kr and the substrate Rayleigh modes. Finally, the dispersion curve of the 25-monolayer Kr film in Fig. 3(d) exhibits a well-developed Rayleigh mode characteristic of the surface of semi-infinite crystals, similar to those already observed for thick films of Kr/Ag(111) (Ref. 5) and Xe/Pt(111).⁶ There is of course no anomaly in this curve, both because of the lack of coupling with the substrate due to the film thickness and because there is no intersection with the substrate Rayleigh wave. Hall, Mills, and Black⁷ have predicted that an additional anomaly should appear at the intersection of the Kr mode with the longitudinal bulk band edge of the substrate [dashed line in Fig. 3(a)], due to the van Hove singularity of the projected density of states of the substrate bulk phonons. In spite of looking carefully in steps of $Q = 0.02 \text{ \AA}^{-1}$ in this

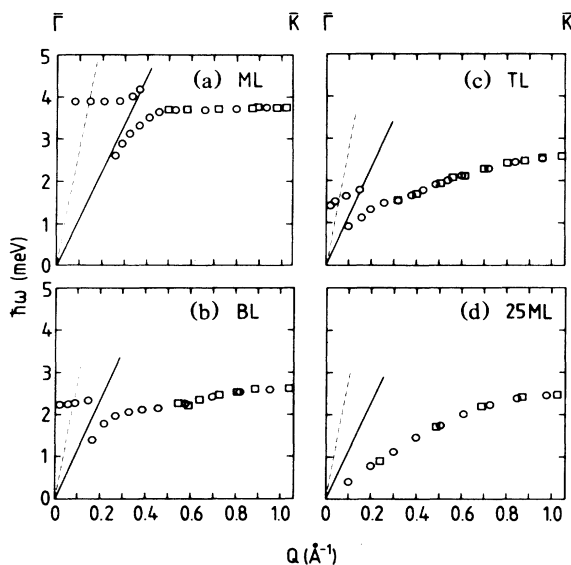


FIG. 3. Experimental dispersion curves of one phonon processes of Kr films (a) ML, (b) BL, (c) TL, and (d) 25 ML along the $(\bar{\Gamma}\bar{K})_{\text{Kr}}$ azimuth. The circles and squares represent phonon creation and annihilation events, respectively. The solid line is the clean Pt(111) Rayleigh phonon dispersion curve and the dashed line the longitudinal bulk band edge of the Pt(111) substrate both in the $(\bar{\Gamma}\bar{M})_{\text{Pt}}$ azimuth (taken from Ref. 11) which is coincident with the $(\bar{\Gamma}\bar{K})_{\text{Kr}}$ azimuth.

range, no indication for this anomaly was observed.

The linewidth broadening as a function of the wave vector Q is shown in Fig. 4 for the mono-, bi-, and trilayer films. As a measure of the linewidth broadening we have plotted $\Delta\varepsilon = [(\delta E)^2 - (E_I)^2]^{1/2}$, where δE and E_I are the full width at half maximum of the major loss feature and of the intrinsic instrumental broadening ($E_I = 0.38 \text{ meV}$ in the present experiment), respectively. The widths have been obtained by Gaussian fitting of the peaks showing up in spectra of the type shown in Fig. 2. The monolayer plot exhibits a substantial linewidth broadening ($\Delta\varepsilon \approx 0.55 \text{ meV}$) in the first third of the BZ. As predicted by Hall, Mills, and Black⁷ the broadening is a consequence of the radiative-damping-induced lifetime shortening due to the coupling with the substrate bulk phonons. The broadening is present, indeed, only in the part of the BZ, where the Kr mode overlaps the projected substrate bulk phonon bands. With increasing wave vector, the Kr mode leaves the bulk bands and the linewidth drops rather abruptly; the width of the Kr phonon peak becomes indistinguishable from the instrumental width. A similar behavior, even if somewhat attenuated, is seen in the bilayer plot, while the trilayer plot shows no evidence for additional broadening due to the coupling with the substrate bulk bands. Note in addition, that at variance with the monolayer case, the bi- and trilayer linewidths exhibit a significant residual broadening ($\Delta\varepsilon \approx 0.2 \text{ meV}$) up to the BZ boundary. Because in this range no coupling with substrate phonons is possible, this broadening is probably due to the coupling with other adsorbate modes.

In summary, the adsorbate-substrate vibrational coupling appears to have a marked influence on the dynamical behavior of physisorbed overlayers. A significant phonon anomaly has been observed for mono-, bi-, and trilayer films of Kr physisorbed on Pt(111), where the adlayer

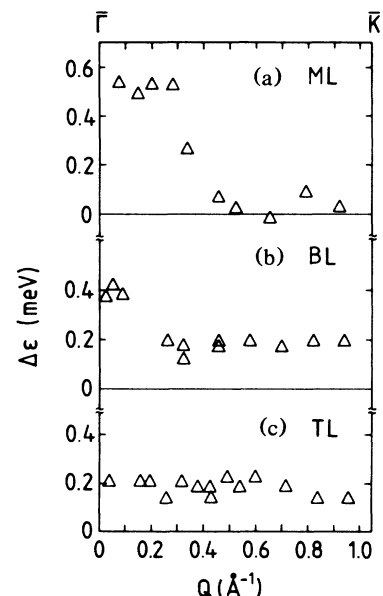


FIG. 4. Measured linewidth broadening $\Delta\varepsilon$ of the Kr creation phonon peaks (a) ML, (b) BL, and (c) TL (see text).

mode intersects the substrate Rayleigh wave. Radiative damping near the zone center, by which the adlayer vibrations decay through emission of phonons to the substrate, has been found to be substantial for mono- and bilayer films. However, we have seen no evidence for a van Hove-type anomaly, which was expected to occur at the crossover between the adlayer mode and the longitudinal bulk band edge of the substrate.

Besides the obvious impact on the lattice dynamics of

physisorbed overlayers, one of the consequences of this study may concern the investigations of the statistical mechanics and thermodynamics of multilayer adsorption. In these studies, the influence of the substrate on bilayer or even thicker layers has to be considered.

Finally, these experiments illustrate that high-resolution inelastic He scattering provides detailed and quantitative information on the dynamical coupling in adsorbate-substrate systems.

¹J. C. Ariyaus, D. L. Mills, K. G. Lloyd, and J. C. Hemminger, *Phys. Rev. B* **30**, 507 (1984).

²P. Avouris and B. N. J. Persson, *J. Phys. Chem.* **88**, 837 (1984).

³J. W. Gadzuk, *J. Electron Spectrosc. Relat. Phenom.* **38**, 233 (1986), and references therein.

⁴B. F. Mason and R. B. Williams, *Phys. Rev. Lett.* **46**, 1138 (1981).

⁵K. D. Gibson and S. J. Sibener, *Phys. Rev. Lett.* **55**, 1514 (1985).

⁶K. Kern, R. David, R. L. Palmer, and G. Comsa, *Phys. Rev. Lett.* **56**, 2823 (1986).

⁷B. M. Hall, D. L. Mills, and J. E. Black, *Phys. Rev. B* **32**, 4932 (1985).

⁸K. D. Gibson and S. J. Sibener, *Faraday Discuss. Chem. Soc.* **80**, 203 (1985).

⁹R. David, K. Kern, P. Zeppenfeld, and G. Comsa, *Rev. Sci. Instrum.* **57**, 2771 (1986).

¹⁰B. Poelsema, R. L. Palmer, G. Mechttersheimer, and G. Comsa, *Surf. Sci.* **117**, 60 (1982).

¹¹K. Kern, R. David, R. L. Palmer, G. Comsa, and T. S. Rahman, *Phys. Rev. B* **33**, 4334 (1986).

¹²K. Kern, P. Zeppenfeld, R. L. Palmer, R. David, and G. Comsa, *Phys. Rev. Lett.* **57**, 3187 (1986).